COMPDYN 2015
5th ECCOMAS Thematic Conference on
Computational Methods in Structural Dynamics and Earthquake Engineering
M. Papadrakakis, V. Papadopoulos, V. Plevris (eds.)
Crete Island, Greece, 25–27 May 2015

EARTHQUAKE LOSS ASSESSMENT OF STEEL FRAME BUILDINGS DESIGNED IN HIGHLY SEISMIC REGIONS

Seong-Hoon Hwang[1], Ahmed Elkady[1], Samy Al.Bardaweel[2] and Dimitrios G. Lignos[1]

[1] McGill University
817 Sherbrooke West, Montreal, Quebec, Canada, H3A 2K6
e-mail: seong-hoon.hwang@mail.mcgill.ca, ahmed.elkady@mail.mcgill.ca, dimitrios.lignos@mcgill.ca

[2] The Lane Construction Corporation
Waco, Texas, USA
samy.albardaweel@mail.mcgill.ca

Keywords: Loss Assessment, Steel Special Moment Frames, Special Concentrically Braced Frames, Losses due to Demolition, Collapse.

Abstract. *In recent years, there is an increasing need to quantify earthquake-induced losses throughout the expected life of a building in order to evaluate alternative design options and to minimize repairs in the aftermath of an earthquake. For this reason, the next generation of performance-based earthquake engineering evaluation procedures has formalized procedures that assess several metrics of seismic performance including economic losses. This paper discusses an analytical study that quantifies the expected earthquake-induced losses in typical office steel buildings designed with perimeter special moment frames or perimeter concentrically braced frames at various ground motion intensities. These buildings are designed in urban California in accordance with today's seismic design provisions in North America. The expected economic losses associated with repair are computed based on a refined performance-based earthquake engineering framework developed within the Pacific Earthquake Engineering Research (PEER) center. This framework integrates site-specific seismic hazard, state-of-the-art nonlinear models that incorporate complex deteriorating phenomena of the structural components of a steel frame building, fragility curves of structural and non-structural components that express the probability of being or exceeding a specific damage level, and the resulting repair costs. The effect of residual deformations along the height of steel frame buildings on their earthquake losses is also examined. It is shown that repair costs in the aftermath of earthquakes vary significantly depending on the employed lateral load resisting system, as well as the analytical model representation of the steel frame building itself.*

1 INTRODUCTION

The next generation of performance-based earthquake engineering (PBEE) procedures [1,2] has formalized a framework for assessing the seismic performance of frame buildings through collapse that was established within the Pacific Earthquake Engineering Research Center (PEER) [3]. The same framework can be employed to assess earthquake-induced losses in buildings [4]. This is particularly important for stakeholders and building owners in order to take informed decisions for effective designs that minimize such losses in the aftermath of an earthquake. In building-specific earthquake loss assessment a numerical model representation of the building is typically subjected to a number of ground motions and critical engineering demand parameters (EDPs) associated with structural and non-structural damage are computed. Such EDPs are related with different damage states of each component of the building such that when these components are repaired their undamaged state is restored. Earthquake-induced losses are calculated through component-based fragility functions that express the probability of exceedance of a component being into a damage state given an EDP of interest (e.g., story drift ratio, absolute floor accelerations). A number of researchers introduced the first generation of building-specific loss estimation methodologies [5–7] that was later refined within PEER including a number of studies associated with earthquake-induced losses in reinforced concrete (RC) and wood structures [8, 9]. More recently, Ramirez and Miranda [10] introduced the influence of residual story drift ratios on building-specific earthquake-induced losses. They indicated that losses in RC frame buildings designed according to modern seismic provisions in highly seismic regions in United States are dominated by residual story drift ratios. This could be a fundamental issue in the case of mid- to high-rise steel frame buildings that utilize perimeter steel special moment frames (SMFs) or special concentrically braced frames (SCBFs). Figure 1 shows a 2-story steel building from the 2011 Tohoku earthquake in Japan that although it did not collapse it still had to be demolished due to excessive residual deformations in its second story after the earthquake. Another interesting aspect of the same problem is the effect of the numerical model that is typically employed to conducted the structural analysis and compute the critical EDPs of interest that are employed to compute the expected losses of a building under a seismic event. To the best of our knowledge, both issues have never been addressed in prior studies associated with building-specific economic losses in the aftermath of an earthquake.

Figure 1: Example of a steel building with residual displacements leading to demolition (source from [11]).

This paper employs a building-specific loss estimation methodology that was originally developed by Ramirez and Miranda [10] that explicitly considers the effect of residual defor-

mations along the height of frame buildings on the economic loss estimation after a seismic event. Low- and mid-rise steel frame buildings with perimeter SMFs and SCBFs designed in urban California are utilized to first compute their expected earthquake-induced losses for various seismic intensities from the onset of structural damage through dynamic collapse. The effect of different analytical model representations of the steel frame buildings on their earthquake-induced losses is also assessed. Two loss metrics are employed for this purpose including the expected losses conditioned on the seismic intensity *IM=im* and the expected annual losses (*EAL*) that provide information to compare to annual insurance premiums, assuming no deductible.

2 OVERVIEW OF LOSS ESTIMATION METHODOLOGY

This section presents a summary of the main aspects of the employed loss estimation methodology adopted by Ramirez and Miranda [10] considering the three possible outcomes for a building after an earthquake, namely (a) collapse does not occur and structural and/or non-structural damage in the building is repaired; (b) collapse does not occur, but the building is demolished and rebuilt; (c) collapse occurs and the building is rebuilt. Assuming that these outcomes are mutually exclusive, then the expected value of the loss in the building for a given seismic intensity *IM* can be computed as follows,

$$E\left[L_T\middle|IM\right]=E\left[L_T\middle|NC\cap R,IM\right]P\left(NC\cap R\middle|IM\right)+E\left[L_T\middle|NC\cap D\right]P\left(NC\cap D\middle|IM\right)+E\left[L_T\middle|C\right]P\left(C\middle|IM\right) \quad (1)$$

where, $E[L_T \mid NC\cap R,IM]$ is the expected value of the total loss in the building given that collapse does not occur and the building is repaired given that the seismic intensity was *IM=im*; $E[L_T \mid NC\cap D]$ is the expected loss in the building when there is no collapse but the building is demolished given that the seismic intensity was *IM=im*; and $E[L_T \mid C]$ is the expected loss in the building when collapse occurs given that the seismic intensity was *IM=im* and corresponds to the cost of removing the building from the site plus the replacement cost of the building. Moreover, $P(NC\cap R \mid IM)$, $P(NC\cap D \mid IM)$ and $P(C \mid IM)$ are the probability that the building will not collapse but that it will be repaired, the probability that the building will not collapse but it will be demolished due to large residual deformations and the probability that the building will collapse given that the seismic intensity of the earthquake is *IM=im*. Equation (1) can be rewritten as follows,

$$\begin{aligned}E\left[L_T\middle|IM\right]=&E\left[L_T\middle|NC\cap R,IM\right]P\left(R\middle|NC,IM\right)P\left(NC\middle|IM\right)\\&+E\left[L_T\middle|NC\cap D\right]P\left(D\middle|NC,IM\right)P\left(NC\middle|IM\right)+E\left[L_T\middle|C\right]P\left(C\middle|IM\right)\end{aligned} \quad (2)$$

where, $P(R \mid NC,IM)$, $P(NC \mid IM)$ are the probability that the building will be repaired given that no collapse occurred and the probability that the building did not collapse, respectively, given a seismic intensity *IM=im*; $P(D \mid NC,IM)$ is the probability that the building will be demolished given that it has not collapsed when subjected to an earthquake with seismic intensity *IM=im*. Equation (2) becomes,

$$\begin{aligned}E\left[L_T\middle|IM\right]=&E\left[L_T\middle|NC\cap R,IM\right]\left\{1-P\left(D\middle|NC,IM\right)\right\}\left\{1-P\left(C\middle|IM\right)\right\}\\&+E\left[L_T\middle|NC\cap D\right]P\left(D\middle|NC,IM\right)\left\{1-P\left(C\middle|IM\right)\right\}+E\left[L_T\middle|C\right]P\left(C\middle|IM\right)\end{aligned} \quad (3)$$

In order to estimate the probability that the building will be demolished given that it has not collapsed when subjected to an earthquake with seismic intensity *IM=im* the following relation can be employed,

$$P\left(D\middle|NC,IM\right)=\int_0^\infty P\left(D\middle|RSDR\right)dP\left(RSDR\middle|NC,IM\right) \tag{4}$$

where, $P(D|RSDR)$ is the probability of having to demolish the building conditioned on the maximum residual story drift ratio (*RSDR*) from all stories of the building; $P(RSDR|NC,IM)$ is the probability of experiencing a certain level of *RSDR* in the building given that it has not collapsed and that it has been subjected to an earthquake with seismic intensity $IM=im$. We have assumed that $P(D|RSDR)$ is lognormally distributed with a median of 0.015 and a logarithmic standard deviation of 0.3 as suggested in [10]. This value is purely based on engineering judgment.

3 DESCRIPTION OF CASE-STUDY STEEL FRAME BUILDINGS

In order to quantify the earthquake-induced losses in steel frame buildings with perimeter SMFs and SCBFs, four steel buildings were considered whose seismic response was thoroughly studied through collapse in prior analytical studies [12–15]. In particular, the four steel buildings are as follows: 4- and 12-story steel frame buildings with perimeter SMFs [12–14]; 3- and 12-story steel frame buildings with perimeter SCBFs [15]. All four buildings were assumed to be located in the Bulk Center (34.000°N, 118.150°W) in Los Angeles, which is considered to be a representative location in urban California with high-seismicity [16]. A seismic design category D_{max} and soil class D is considered. The site-specific seismic hazard curves for the four steel buildings considered as part of this paper are shown in log-log scale in Figure 2. All the buildings were designed in accordance with ASCE-7-10 [17], ANSI/AISC 341-10 [18] seismic provisions. A plan view and elevation of a typical 4- and 3-story steel frame building with perimeter SMFs and SCBFs, respectively, are shown in Figure 3. The steel SMFs utilize typical fully restrained beam-to-columns connections with reduced beam sections (RBS) designed according to AISC-358-10 [19]. Details regarding the design of these buildings are summarized in [12–14]. The SCBFs utilize round steel hollow structural sections as braces as discussed in [15]. Their gusset plates have been designed according to a balanced design approach proposed by Lehman et al. [20]. Note that for the 3-story steel frame building with SCBFs only two SCBFs were designed per loading direction (see Figure 3c). The interior gravity framing (i.e., floor system and gravity columns) of the four steel frame buildings was explicitly designed based on ANSI/AISC-360-10 [21]. Note that the orientation of the strong axis of the interior gravity columns is assumed to be perpendicular to the loading direction of interest [i.e., east-west (EW)] as shown in Figures 3a and 3c.

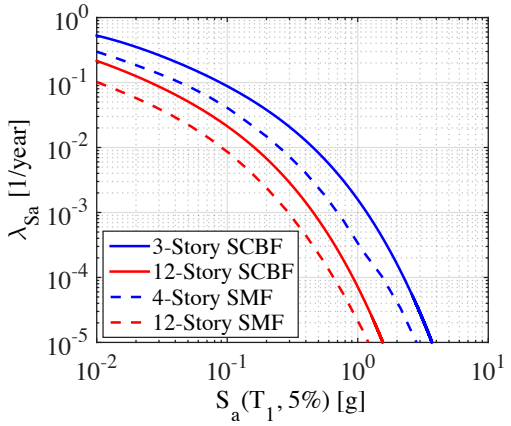

Figure 2: Site-specific hazard curves for the four steel buildings considered.

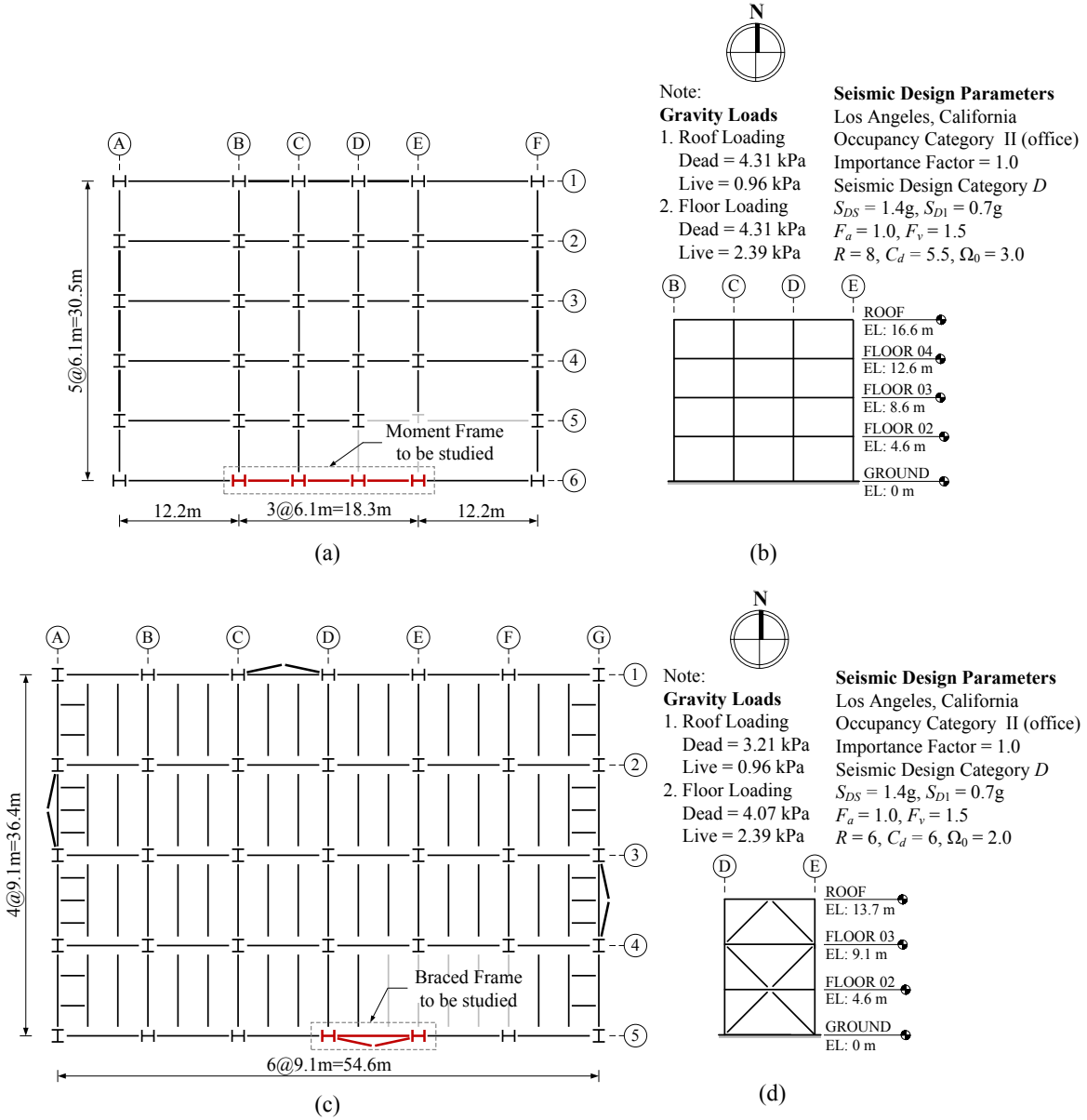

Figure 3: Typical office steel buildings with perimeter steel SMFs and SCBFs.

3.1 Fragility and cost distribution functions

In order to compute realistic loss estimations for the steel frame buildings being considered architectural layouts are developed. A rectangular footprint that is 1,296.25m^2 (14,000 sq.ft) and 1,871.36m^2 (20,144 sq.ft) is developed for the steel frame buildings with perimeter SMFs and SCBFs, respectively (see Figures 3a and c). Prior studies by Aslani and Miranda [22] have demonstrated that a large contributor to earthquake-induced losses in frame buildings is the damage to their nonstructural components even for moderate seismic intensities. The replacement cost estimates for the four buildings that were studied as part of this paper are summarized in Table 1. These replacement cost estimates are employed to normalize the expected losses for the four steel frame buildings at various seismic intensities as discussed later on in Section 5.Cost estimates were developed using the RS Means Cost Estimating Manuals [23] and listed in Table 2 based on the considered damageable components (structural and nonstructural) together with the fragility distribution functions assigned with the repair of the-

se components. Note that the source for each component fragility curve is also noted as part of Table 1.

Building type	Footprint	Area [m^2]	Replacement cost ($)	Cost per m^2 ($)
4-story with perimeter SMFs	42.5m x 30.5m	5,185	7,000,000	1350.1
12-story with perimeter SMFs	42.5m x 30.5m	15,555	21,000,000	1350.1
3-story with perimeter SCBFs	36.4m x 54.4m	5,614	8,100,000	1442.8
12-story with perimeter SCBFs	36.4m x 54.4m	22,456	32,400,000	1442.8

Table 1: Cost estimates for steel frame buildings studied

Assembly description	Damage state	Fragility parameters			Repair cost parameters	
		EDP	x_m	beta	x_m ($)	beta
Columns (base plate) [1,2]	Crack Initiation	SDR (unitless)	0.04	0.40	19224	0.41
	Crack Propagation		0.07	0.40	27263	0.37
	Fracture		0.10	0.40	32424	0.34
Columns (splices) [1,2]	Cracking of the groove welded flange	SDR (unitless)	0.04	0.4	9445	0.32
	Column web failure		0.07	0.4	11246	0.30
	Fracture		0.10	0.4	38473	0.17
Round HSS Braces (Brace weight < 40 plf) [24]	Brace flexural buckling	SDR (unitless)	0.0041	0.51	30897	0.33
	Brace local buckling		0.0096	0.45	39438	0.30
	Brace strength loss		0.0275	0.51	39438	0.30
Round HSS Braces (41 plf < Brace weight < 99 plf) [24]	Brace flexural buckling	SDR (unitless)	0.0041	0.51	30897	0.33
	Brace local buckling		0.0096	0.45	54892	0.28
	Brace strength loss		0.0275	0.51	54892	0.28
Non-RBS beam-column moment connections (beam depth <= W27) [1,2]	Local buckling	SDR (unitless)	0.03	0.30	16033	0.35
	lateral-torsional buckling		0.04	0.30	25933	0.31
	fracture		0.05	0.30	25933	0.31
Non-RBS beam-column moment connections (beam depth >= W30) [1,2]	Local buckling	SDR (unitless)	0.03	0.30	17033	0.33
	lateral-torsional buckling		0.04	0.30	28433	0.28
	fracture		0.05	0.30	28433	0.28

Table 2: fragility and cost distributions.

RBS beam-column moment connections (One side of beam) [25]	Yield Anywhere	SDR (unitless)	0.01	0.17	0	0
	Yielding First in Panel Zone	SDR (unitless)	0.01	0.15	0	0
	Yielding First in Flange	SDR (unitless)	0.0096	0.10	0	0
	Local Buckling	SDR (unitless)	0.0216	0.30	16033	0.352
	Fracture	SDR (unitless)	0.05	0.30	26000	0.305
RBS beam-column moment connections (Both sides of beam) [25]	Yield Anywhere	SDR (unitless)	0.01	0.17	0	0
	Yielding First in Panel Zone	SDR (unitless)	0.01	0.15	0	0
	Yielding First in Flange	SDR (unitless)	0.0096	0.10	0	0
	Local Buckling	SDR (unitless)	0.0216	0.30	24000	0.33
	Fracture	SDR (unitless)	0.05	0.30	41840	0.27
Shear tab connections [1,2]	Yielding of shear tab	SDR (unitless)	0.04	0.40	12107	0.37
	Partial tearing of shear tab		0.08	0.40	12357	0.38
	Complete separation of shear tab		0.11	0.40	12307	0.38
Corrugated Slab (90mm steel; 100mm overlay) [26]	Crack Initiation	SDR (unitless)	0.00375	0.13	18	0.35
	Crushing Near Column		0.01	0.22	33	0.35
	Shear Stud Fracture		0.05	0.35	57	0.35
Drywall partition [1,2]	Visible	SDR (unitless)	0.0039	0.17	90	0.20
	Significant	SDR (unitless)	0.0085	0.23	530	0.20
Drywall finish [1,2]	Visible	SDR (unitless)	0.0039	0.17	90	0.20
	Significant	SDR (unitless)	0.0085	0.23	250	0.20
Acoustic ceiling [1,2]	Collapse	PFA(g)*	92/(l+w)	0.81	2.2×A	0.50
Automatic sprinklers [1,2]	Fracture	PFA(g)*	0.32	1.40	900	0.50
Elevators [1,2]	Failure	PGA(g)+	0.41	0.28	5000	1.00

*PFA: Peak floor absolute acceleration (units of g); + PGA: Peak ground acceleration (units of g)

Table 2 (continued): fragility and cost distributions.

4 NONLINEAR BUILDING MODELS AND COLLAPSE SIMULATIONS

Nonlinear analytical model representations of the steel frame buildings discussed in Section 3 are developed in the OpenSees simulation platform [27]. These models are 2-Dimensional (2-D). In order to assess the effect of the analytical model representation of a steel building on its loss estimation due to earthquake shaking two types of analytical models are developed. The first one is a model that considers the bare steel structural components of the corresponding lateral load resisting system (i.e., bare SMF and bare SCBF: noted as B-model); the second one is a model that considers the effects of the composite slab and the interior gravity framing system on the lateral strength and flexural stiffness of the steel frame building under consideration (noted as CG model).

The SMF steel beams and columns are modeled with concentrated plasticity hinges (i.e., lumped plasticity) employing a phenomenological deterioration model that was developed by Ibarra et al. [28] and was further refined and calibrated by Lignos and Krawinkler [29] with a comprehensive steel beam database [30] (publically available from the following link: http://dimitrios-lignos.research.mcgill.ca/databases/). In order to take into consideration the effect of composite action on the hysteretic response of the beams with RBS modeling recommendations by Elkady and Lignos [13] are employed. Figure 4a shows a comparison of the simulated and measured moment-rotation hysteretic relation of a fully restrained beam-to-column connection with RBS including the composite action. The effect of gravity framing on the overall seismic performance of steel frame buildings is captured as discussed in Elkady and Lignos [14]. This necessitates a realistic representation of typical shear-tab beam-to-column connections that are used for the design of the floor system of a steel frame building. Figure 4b illustrates a comparison of the measured and simulated moment-rotation hysteretic relation of a shear-tab beam-to-column connection including the possibility of beam binding on the column flange as discussed in [14].

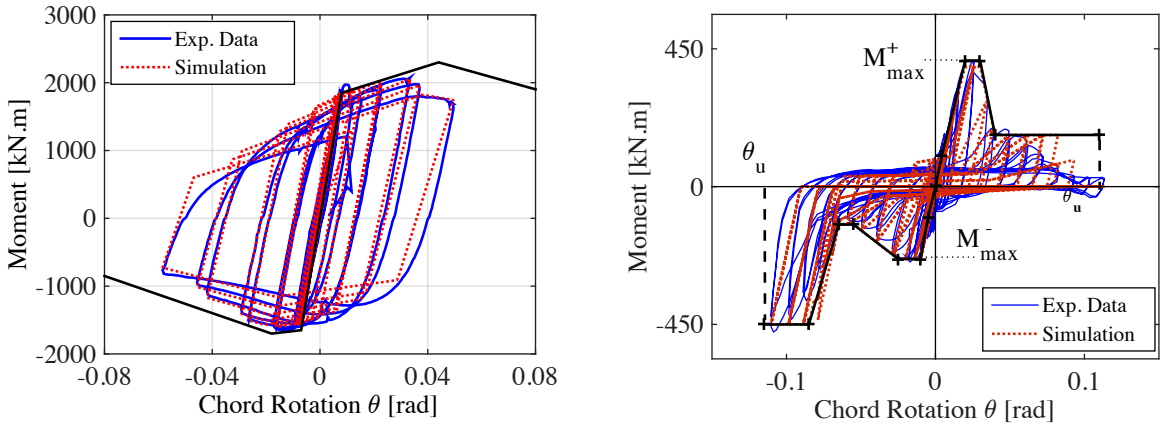

Figure 4: Examples of modeling the moment-rotation hysteretic relation of fully-restrained beam-to-column connections with RBS and typical single-row shear tab beam-to-column connections (data from [30,31])

The SCBFs are modeled based on the computational approach discussed in Karamanci and Lignos [33]. In summary, steel braces are modeled with fiber-based elements that are able to trace flexural buckling as well as fracture initiation due to low-cycle fatigue based on the material model proposed by Uriz et al. [34]. Figure 5a illustrates a comparison of the measured and simulated hysteretic axial force-axial deformation relation of a round HSS steel brace based on the approach discussed in Karamanci and Lignos [33,35]. The flexibility and flexural yielding of the gusset plates at the ends of the steel braces due to out-of-plane brace deformations is explicitly considered based on the model proposed by Hsiao et al. [36]. Cyclic

deterioration in flexural strength and stiffness of SCBF beams and columns are simulated based on the approach discussed earlier for SMFs.

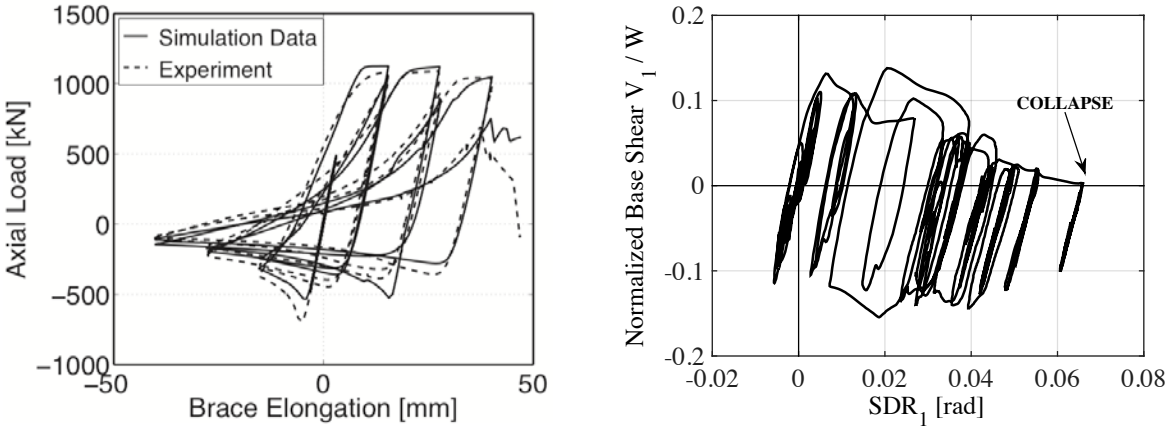

(a) modeling inelastic buckling and fracture in steel braces (b) definition of sidesway collapse

Figure 5: Modeling inelastic buckling and fracture in steel braces and definition of sidesway collapse in steel frame buildings (data from [37]).

The analytical model representations of the steel frame buildings discussed earlier are subjected to the Far-Field set of 44 ground motions from FEMA P695 [37]. This set represents large magnitude earthquakes, recorded on rick or stiff soil sites and they represent the seismic hazard of the design location. Incremental dynamic analysis (IDA) is employed as discussed by Vamvatsikos and Cornell [39] in order to trace the dynamic collapse due to sidesway instability for each analytical model. Collapse occurs when a story or a number of stories displaces sufficiently such that P-Delta effects accelerated by component deterioration make the first-order story shear resistance of the respective model equal to zero. Figure 5b illustrates an example of such case for the CG-model of the 12-story steel frame building with SMFs. This definition of collapse is consistent with prior small and full-scale shake table collapse tests of steel frame buildings [39–41]. The *EDPs* of interest [i.e., peak story drift ratios (*SDRs*), peak absolute floor accelerations (*PFAs*), residual story drift ratios (*RSDRs*)] are obtained for each ground motion over the full range or seismic intensities through collapse. Figures 6a and 6b illustrate the peak *SDRs* and *PFAs* versus *IM* [i.e., $S_a(T_1,5\%)$], respectively, for the 12-story steel frame building with perimeter SMFs (CG-model). In the same figures we have superimposed the counted median, 16th and 84th percentiles based on the set of 44 ground motions. Based on the IDA, a collapse fragility curve is computed per analytical model representation that describes the probability of collapse as a function of the first mode spectral acceleration $S_a(T_1,5\%)$. Figure 6c illustrates the collapse fragility curves for the four CG models of the steel frame buildings with perimeter SMFs and SCBFs.

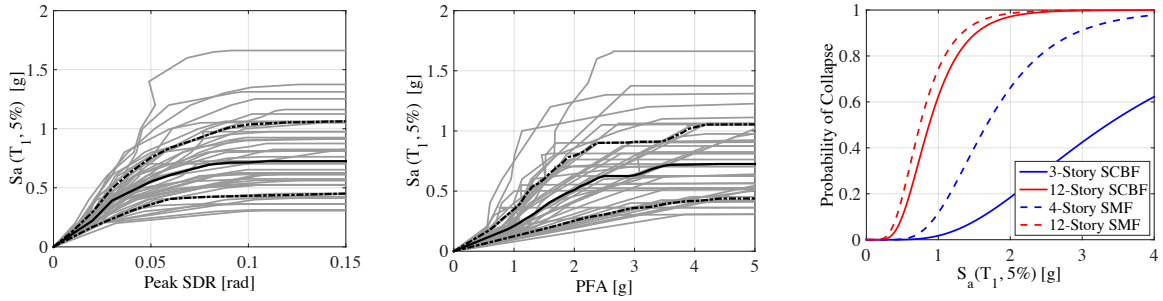

(a) IM versus peak SDRs (b) IM versus PFAs (c) collapse fragility curves

Figure 6: Critical EDPs and collapse fragility curves for steel frame buildings with perimeter SMFs and SCBFs.

5 EXPECTED LOSSES CONDITIONED ON SEISMIC INTENSITY

The expected losses are computed for each building conditioned on the seismic intensity, as shown in Figures 7a and c for the 12-story steel frame buildings with perimeter SMFs and SCBFs, respectively, when the bare frame is only considered as part of the analytical model representation of the building under consideration (i.e., B-models). These curves are also known as loss vulnerability curves [10]. The total repair losses conditioned on seismic intensity are further disaggregated into losses due to structural and nonstructural component repair, losses due to demolition given that building collapse has not occurred and losses due to dynamic collapse. In these figures the expected losses for the 12-story steel frame building are normalized with respect to its total replacement cost (see Table 1). For steel frame buildings with perimeter SMFs (see Figure 7a) the total loss vulnerability curves initially increase linearly with respect to the seismic intensity. Note that for the case of the 12-story steel frame building under service level [i.e., SLE: $S_a(T_1,5\%) = 0.11g$] and design level [i.e., DLE: $S_a(T_1,5\%) = 0.32g$] earthquake intensities losses are dominated by damage into nonstructural components (see Figure 7b). This is to be expected based on past reconnaissance reports for steel buildings with moment resisting frames [42,43]. However, from Figure 7c, this is not the case for steel frame buildings with perimeter SCBFs. In particular, under the DLE intensity [i.e., $S_a(T_1,5\%) = 0.40g$] the expected losses equal to the 20% of the replacement cost of the 12-story steel building with SCBFs is attributed to damage due to flexural buckling of its steel round HSS braces (see Figure 7d). This is to be expected due to the fact that steel braces would typically buckle in flexure at about 0.5% story drift ratios as discussed in Lignos and Karamanci [24]. From Figure 7 losses are dominated by the non-collapse losses at lower intensities that have a higher rate of occurrence regardless of the lateral load resisting system. From the same figure, for seismic intensities higher than 0.4g that are associated with maximum considered earthquakes (i.e., MCE: 2% probability of exceedance over 50 years) collapse losses tend to contribute much more to the overall earthquake-induced losses of a steel frame building regardless of its height and its lateral load resisting system. This can be clearly seen in Figures 7b and 7d. From the same figures, another notable observation is that at higher seismic intensities associated with MCE shaking building losses are dominated by demolition given that building collapse has not occurred. This is much more evident for the 12-story steel building with SMFs (see Figure 7b) compared to the 12-story steel building with SCBFs (see Figure 7d). This agrees with earlier findings on code-compliant RC frame buildings [10]. Similar observations hold true for the 4-and 3-story steel frame buildings with perimeter SMFs and SCBFs, respectively.

In order to examine the effect of analytical model representation of a steel frame building on its earthquake loss estimation the same analysis discussed above is repeated for the CG models (see Section 4). Figures 8a and 8c illustrate the loss vulnerability curves for the 12-story steel buildings with perimeter SMFs and SCBFs, respectively, when the gravity framing is considered as part of the analytical model of the respective building. From these figures, the findings associated with (a) the magnitude of earthquake losses and (b) the primary contributors to total losses for low seismic intensities (i.e., SLE, DLE) are practically the same with the ones computed based on the B-models building representations. This can be seen in Figures 8b and 8d for the 12-story steel frame with perimeter SMFs and SCBFs, respectively. It is worth mentioning that for the 12-story building with perimeter SMFs for seismic intensities associated with extreme earthquake events (i.e., MCE intensity) the losses due to demolition become nearly half compared to estimated ones based on the B-model of the same building (see Figure 8b). Losses associated with collapse are also reduced by about 50% as shown in Figure 8b in comparison with Figure 7b (i.e., results are based on the B-model). Similarly, for

the 12-story steel building with perimeter SCBFs losses due to demolition become very small under a MCE seismic intensity as shown in Figure 8d. This indicates that there is less drift concentration in the bottom stories of steel frame buildings with SCBFs when the interior gravity framing is considered as part of the lateral-force resistance system. This agrees with findings from prior analytical studies on braced frames [45]. Note that for $S_a(T_1,5\%) > 0.7g$ losses due to demolition become fairly large the 12-story steel frame building with perimeter SCBFs. However, losses due to collapse practically are not affected by the analytical model representation of the same building. This is attributed to the fact that in concentrically braced frames it is nearly impossible to achieve a uniform demand-to-capacity ratio along their height and ultimately avoid local story mechanisms that are associated with concentration of plastic deformations that trigger structural collapse [33].

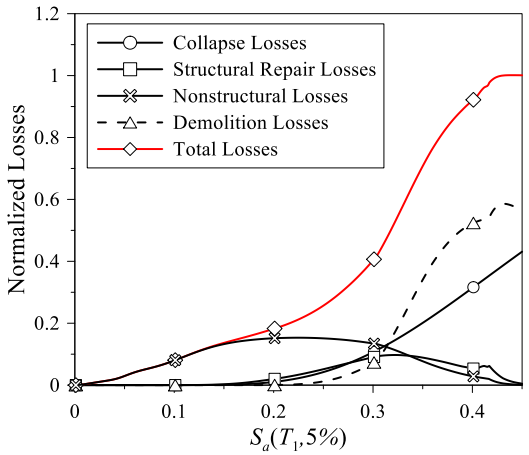

(a) 12-story steel building with SMFs

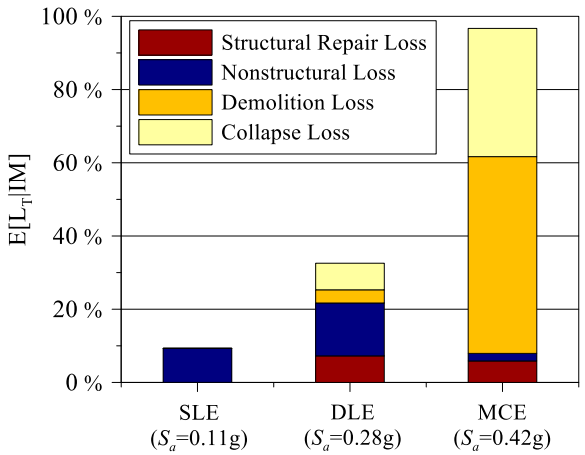

(b) 12-story steel building with SMFs-three intensities

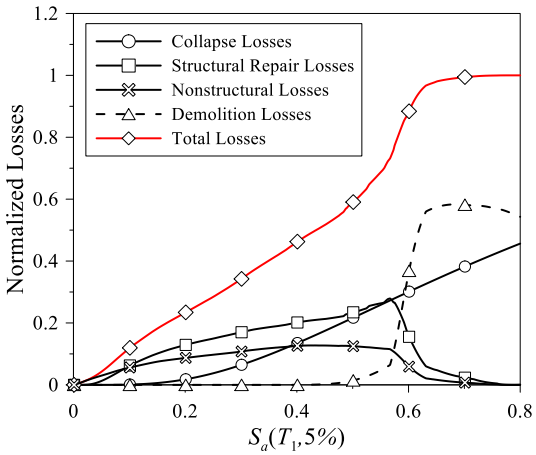

(c) 12-story steel building with SCBFs

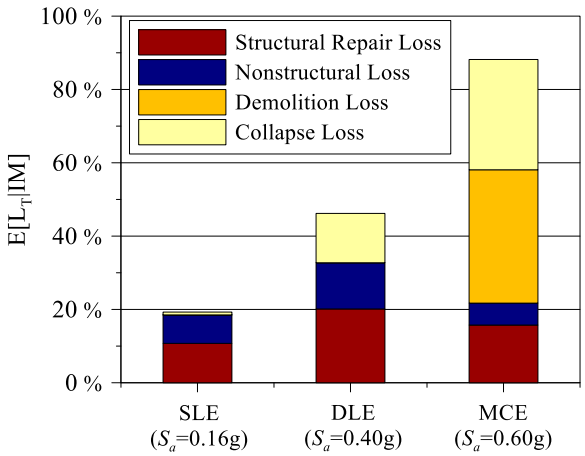

(d) 12-story steel building with SCBFs-three intensities

Figure 7: Normalized loss vulnerability functions for steel frame buildings with perimete SMFs and SCBFs conditioned on seismic intensity without considering the gravity framing system and composite action as part of the analytical model representation (B-models)

In summary, from a comparison of Figures 7 and 8 it is clear that earthquake induced losses in steel frame buildings may be significantly overestimated under MCE seismic intensities if the contribution of the interior gravity framing and the composite action to lateral strength and stiffness is neglected.

6 EXPECTED ANNUAL LOSSES

This section summarizes the normalized *EAL* results for the four steel frame buildings that are studied depending on the employed analytical model representation (i.e., B-models versus CG models). The *EAL* is computed as follows,

$$E\left(L_T\right)=\int_0^{\infty}E\left(L_T\middle|IM\right)\mathrm{d}\lambda\left(IM\right)=\int_0^{\infty}E\left(L_T\middle|IM\right)\left|\frac{\mathrm{d}\lambda\left(IM\right)}{\mathrm{d}IM}\right|\mathrm{d}IM \tag{5}$$

where $\lambda(IM)$ is the mean annual frequency of the ground motion intensity and $|\mathrm{d}\lambda(IM)/\mathrm{d}(IM)|$ is the derivative of the seismic hazard curve (see Figure 2).

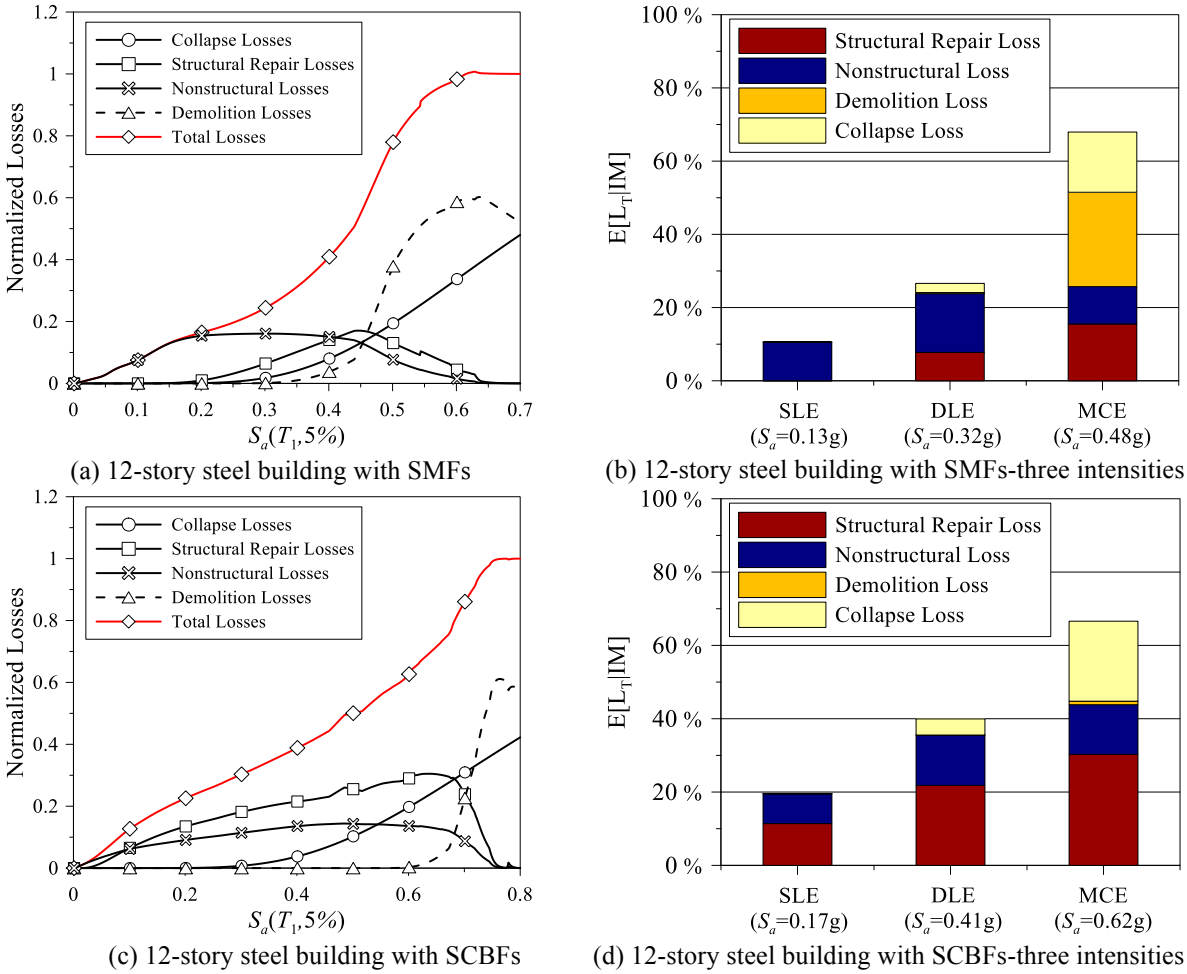

(a) 12-story steel building with SMFs

(b) 12-story steel building with SMFs-three intensities

(c) 12-story steel building with SCBFs

(d) 12-story steel building with SCBFs-three intensities

Figure 8: Normalized loss vulnerability functions for steel frame buildings with perimeter SMFs and SCBFs conditioned on seismic intensity based on analytical mode representations that include the gravity framing system (CG-models).

Figure 9a illustrates the normalized *EAL* results for the 4- and 12-story steel frame buildings with perimeter SMFs. Based on this figure the expected annual losses vary between 0.41 to 0.67% of the replacement costs for mid-rise and low-rise steel buildings, respectively. The total normalized annual losses for the 3- and 12-story steel frame buildings with perimeter SCBFs tend to be larger than the equivalent results for steel frame buildings with SMFs as shown in Figure 9b. In order to explain this finding the *EAL* results are further disaggregated into losses due to acceleration- and drift-sensitive nonstructural components, structural repair and demolition losses and collapse losses. For steel frame buildings with perimeter SMFs the

expected annual losses and demolition and collapse expected annual losses. From Figure 9, the drift-sensitive nonstructural components of steel frame buildings with perimeter SMFs contribute more to the total *EAL*s than the equivalent *EAL* results for steel frame buildings with SCBFs. This is to be expected given the flexibility of the former compared to the latter. However, steel frame buildings with perimeter SCBFs tend to have nearly double *EALs* due to acceleration-sensitive nonstructural component repairs compared to steel frame buildings with perimeter SMFs. This is attributed to the fact that SCBFs are typically much stiffer than SMFs with the same height. Another notable observation from Figure 9b is that *EALs* due to structural damage into steel round HSS braces in mid-rise steel buildings with perimeter SCBFs become comparable with *EALs* due to acceleration-sensitive nonstructural component repairs. This is attributed to the relatively small story drift ratios that flexural buckling may occur in steel braces [24]. On the contrary, in steel frame buildings with perimeter SMFs the *EAL* results in terms of repairs of the primary structural components (e.g., beam-to-column connections and/or steel columns) is a negligible fraction of the total *EAL*s. The reason is that such components are typically damaged at story drift ratios larger than 1%.

It is worth mentioning that *EAL* results weight all possible levels of seismic intensity by taking into account their probability of occurrence (see Eq. 5). Therefore, it may be a more comprehensive loss metric than other loss metrics conditioned on a single seismic intensity such as a service, design or maximum considered earthquake in order to evaluate a steel frame building's seismic risk.

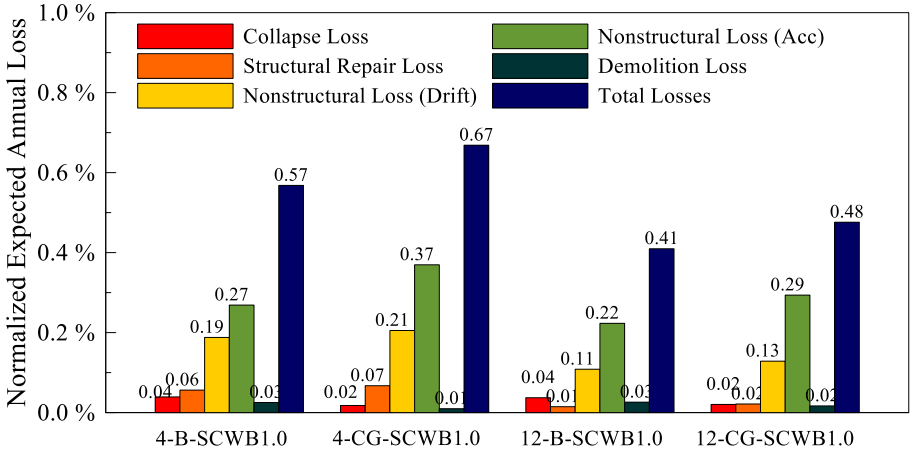

(a) Normalized expected annual losses for steel frame buildings with perimeter SMFs

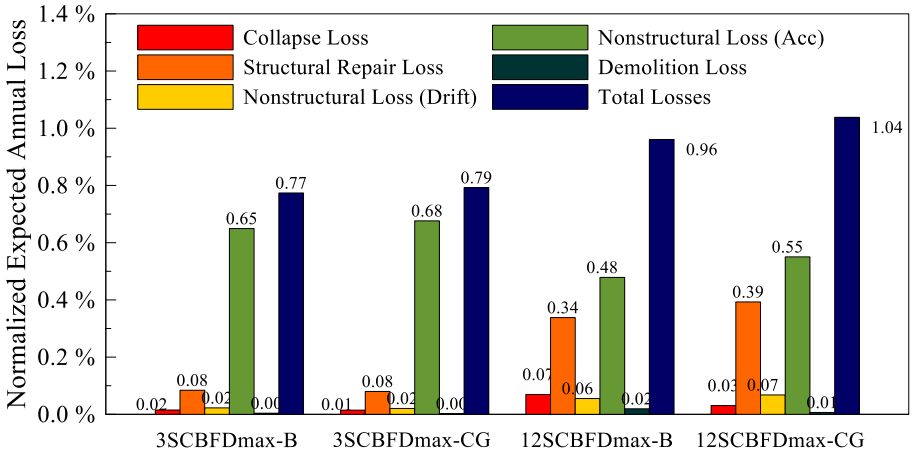

(b) Normalized expected annual losses for steel frame building with perimeter SCBFs

Figure 9: Normalized expected annual losses for steel frame buildings with perimeter SMFs and SCBFs.

7 CONCLUSIONS

This paper evaluated the earthquake-induced losses in four steel frame buildings with perimeter special moment frames (SMFs) and special concentrically braced frames (SCBFs) designed in urban California in accordance with today's regional seismic provisions. Two types of analytical model representations of the steel frame buildings were considered including (a) models that represent the bare structural components of the lateral load resisting system of a building; and (b) models that take into account the composite action and the interior gravity framing of a steel frame building. The earthquake loss assessment was based on two primary loss metrics including (a) the expected losses conditioned on seismic intensity and (b) the expected annual losses. The effect of residual deformations of a building that did not collapse at a given seismic intensity on its earthquake losses was considered based on the approach discussed in [10]. Even though the present assessment is based on four steel frame buildings only, the main findings discussed in this paper are summarized as follows:

- Non-collapse repairs at low seismic intensities associated with service and/or design level earthquakes dominate building earthquake losses. The primary contributor to these losses is damage to the nonstructural content of a building regardless of the selected lateral load resisting system.
- At seismic intensities associated with design level earthquakes, steel buildings that utilize perimeter SCBFs tend to have considerable repairs due to steel brace flexural buckling. This is not the case for steel buildings that utilize perimeter SMFs.
- Demolition and collapse losses tend to dominate building earthquake losses at seismic intensities associated with maximum considered earthquakes. Demolition losses are attributed to large residual deformations that steel frame buildings may experience during a large earthquake.
- Earthquake-induced losses in steel frame buildings may be considerably overestimated when critical engineering demand parameters (EDPs) that control losses are based on analytical models that represent the bare lateral load resisting system only. The consideration of the composite action and the interior gravity framing of a steel frame building in the analytical model representation of a building reduces the earthquake-induced losses due to demolition by more than 50% regardless of the employed lateral load resisting system.
- In steel frame buildings with perimeter SMFs repairs in drift-sensitive nonstructural components followed by acceleration-sensitive nonstructural components primarily dominate the expected annual losses. The expected annual losses in steel frame buildings with perimeter SCBFs are dominated by acceleration-sensitive nonstructural components due to high absolute floor acceleration demands because of the considerable lateral stiffness of a SCBF. An important contributor to the expected annual losses is steel brace repairs due to flexural buckling at fairly small story drift ratios.

REFERENCES

[1] FEMA, "Seismic performance assessment of buildings Volume 1 - Methodology." Federal Emergency Management Agency (FEMA), Washington, DC, 2012.
[2] FEMA, "Seismic performance assessment of buildings, Volume 2 - Implementation Guide." Federal Emergency Management Agency (FEMA), Washington, DC, 2012.

[3] A. Cornell C. and H. Krawinkler, "Progress and challenges in seismic performance assessment.," in *PEER Center News*, Berkeley, California, 2000, vol. 3, pp. 1–4.
[4] H. Krawinkler and E. Miranda, "Performance-based earthquake engineering, Chapter 9," in *Earthquake Engineering: From Engineering Seismology to Performance-Based Engineering*, vol. 1st, 1 vols., Boca Raton, FL: CRC Press, 2004, pp. 9–1 to 9–59.
[5] K. A. Porter, A. S. Kiremidjian, and J. S. LeGrue, "Assembly-based vulnerability of buildings and its use in performance evaluation," *Earthq. Spectra*, vol. 17, no. 2, pp. 291–312, May 2001.
[6] S. Gunturi, "Building-specific earthquake damage estimation," PH.D. Dissertation, John A. Blume Earthquake Engineering Center, Stanford University, Stanford, California, 1993.
[7] A. Singhal and A. Kiremidjian, "A Method for earthquake motion-damage relationships with application to reinforced concrete frames.," John A. Blume Earthquake Engineering Center, Stanford University, Stanford, California, Technical Report 119, 1996.
[8] C. M. Ramirez, A. B. Liel, J. Mitrani-Reiser, C. B. Haselton, A. D. Spear, J. Steiner, G. G. Deierlein, and E. Miranda, "Expected earthquake damage and repair costs in reinforced concrete frame buildings," *Earthq. Eng. Struct. Dyn.*, vol. 41, no. 11, pp. 1455–1475, Sep. 2012.
[9] S. Pei and J. W. van de Lindt, "Methodology for earthquake-induced loss estimation: An application to woodframe buildings," *Struct. Saf.*, vol. 31, no. 1, pp. 31–42, Jan. 2009.
[10] C. M. Ramirez and E. Miranda, "Significance of residual drifts in building earthquake loss estimation," *Earthq. Eng. Struct. Dyn.*, vol. 41, no. 11, pp. 1477–1493, Sep. 2012.
[11] T. Okazaki, D. G. Lignos, M. Midorikawa, J. M. Ricles, and J. Love, "Damage to steel buildings observed after the 2011 Tohoku-Oki earthquake," *Earthq. Spectra*, vol. 29, no. S1, pp. S219–S243, Mar. 2013.
[12] A. Elkady and D. G. Lignos, "Effect of composite action on the dynamic stability of special steel moment resisting frames designed in seismic regions," in *Structures Congress 2013*, pp. 2151–2160.
[13] A. Elkady and D. G. Lignos, "Modeling of the composite action in fully restrained beam-to-column connections: implications in the seismic design and collapse capacity of steel special moment frames," *Earthq. Eng. Struct. Dyn.*, vol. 43, no. 13, pp. 1935–1954, Apr. 2014.
[14] A. Elkady and D. G. Lignos, "Effect of gravity framing on the overstrength and collapse capacity of steel frame buildings with perimeter special moment frames," *Earthq. Eng. Struct. Dyn.*, (available in early view), Nov. 2014.
[15] NIST, "Evaluation of the FEMA P-695 Methodology for Quantification of Building Seismic Performance Factors." National Institute of Standards and Technology (NIST), U.S. Department of Commerce, Gaithersburg, Maryland, 2009.
[16] C. A. Goulet, C. B. Haselton, J. Mitrani-Reiser, J. L. Beck, G. G. Deierlein, K. A. Porter, and J. P. Stewart, "Evaluation of the seismic performance of a code-conforming reinforced-concrete frame building—from seismic hazard to collapse safety and economic losses," *Earthq. Eng. Struct. Dyn.*, vol. 36, no. 13, pp. 1973–1997, Oct. 2007.
[17] ASCE, "Minimum Design Loads for Buildings and Other Structures." American Society of Civil Engineers, Reston, Virginia, 2010.
[18] AISC, "Seismic provisions for structural steel buildings," American Institute for Steel Construction, Chicago, IL, Seismic Provisions ANSI/AISC 341-10, 2010.
[19] AISC, "Prequalified connections for special and intermediate steel moment frames for seismic applications," American Institute for Steel Construction, Chicago, IL, Seismic Provisions ANSI/AISC 358-10, 2010.

[20] D. Lehman, C. Roeder W., D. Herman, S. Johnson, and B. Kotulka, "Improved seismic performance of gusset plate connections," *J. Struct. Eng.*, vol. 134, no. 6, pp. 890–901, 2008.
[21] AISC, "Specification for structural steel buildings," American Institute for Steel Construction, Chicago, IL, Seismic Provisions ANSI/AISC 360-10, 2010.
[22] H. Aslani and E. Miranda, "Probabilistic earthquake loss estimation and loss disaggregation in buildings," John A. Blume Earthquake Engineering Center, Stanford University, Stanford, California, Ph.D. Thesis 157, 2005.
[23] RS Means, *Square foot costs 2015*, 36th ed. Kingston, MA: RS Means Corporation, 2015.
[24] D. G. Lignos and E. Karamanci, "Drift-based and dual-parameter fragility curves for concentrically braced frames in seismic regions," *J. Constr. Steel Res.*, vol. 90, pp. 209–220, Nov. 2013.
[25] D. G. Lignos, D. Kolios, and E. Miranda, "Fragility assessment of reduced beam section moment connections," *J. Struct. Eng.*, vol. 136, no. 9, pp. 1140–1150, 2010.
[26] S. Al Bardaweel and D. G. Lignos, "Indicators for sustainable design of civil engineering systems: Towards earthquake resilient steel frame buildings through loss assessment, Report No. G13-49," Master of Science, McGill University, McGill University, Montreal, Canada, 2013.
[27] F. T. Mckenna, "Object-oriented finite element programming: frameworks for analysis, algorithms and parallel computing," University of California, Berkeley, 1997.
[28] L. F. Ibarra, R. A. Medina, and H. Krawinkler, "Hysteretic models that incorporate strength and stiffness deterioration," *Earthq. Eng. Struct. Dyn.*, vol. 34, no. 12, pp. 1489–1511, Oct. 2005.
[29] D. G. Lignos and H. Krawinkler, "Deterioration Modeling of Steel Components in Support of Collapse Prediction of Steel Moment Frames under Earthquake Loading," *J. Struct. Eng.*, vol. 137, no. 11, pp. 1291–1302, 2011.
[30] D. G. Lignos and H. Krawinkler, "Development and utilization of structural component databases for performance-based earthquake engineering," *J. Struct. Eng.*, vol. 139, no. 8, pp. 1382–1394, 2013.
[31] X. Zhang and J. M. Ricles, "Experimental evaluation of reduced beam section connections to deep columns," *J. Struct. Eng.*, vol. 132, no. 3, pp. 346–357, 2006.
[32] J. Liu and A. Astaneh-Asl, "Cyclic testing of simple connections including effects of slab," *J. Struct. Eng.*, vol. 126, no. 1, pp. 32–39, 2000.
[33] E. Karamanci and D. Lignos G., "Computational approach for collapse assessment of concentrically braced frames in seismic regions," *J. Struct. Eng.*, vol. 15, no. A4014019, pp. 1-15, 2014.
[34] P. Uriz, F. Filippou, and S. Mahin, "Model for cyclic inelastic buckling of steel braces," *J. Struct. Eng.*, vol. 134, no. 4, pp. 619–628, 2008.
[35] D. G. Lignos and E. Karamanci, "Predictive equations for modelling cyclic buckling and fracture of steel braces," in *10CUEE Conference Proceedings*, Tokyo Institute of Technology, Tokyo, Japan, 2013.
[36] P.-C. Hsiao, D. E. Lehman, and C. W. Roeder, "Improved analytical model for special concentrically braced frames," *J. Constr. Steel Res.*, vol. 73, pp. 80–94, Jun. 2012.
[37] B. Fell, A. Kanvinde, G.G. Deierlein, and A. Myers, "Experimental Investigation of Inelastic Cyclic Buckling and Fracture of Steel Braces," *J. Struct. Eng.*, vol. 135, no. 1, pp. 19–32, 2009.
[38] FEMA, "Quantification of Building Seismic Performance Factors." Federal Emergency Management Agency (FEMA), Washington, DC, 2009.

[39] D. Vamvatsikos and C. A. Cornell, "Incremental dynamic analysis," *Earthq. Eng. Struct. Dyn.*, vol. 31, no. 3, pp. 491–514, Mar. 2002.

[40] D. Lignos G., H. Krawinkler, and A. Whittaker S., "Collapse assessment of a 4-story steel moment resisting frame," in *2nd International Conference on Computational Methods in Structural Dynamics & Earthquake Engineering*, Rodos, Greece, 2009.

[41] D. Lignos G., H. Krawinkler, and A. Whittaker S., "Prediction and validation of sidesway collapse of two scale models of a 4-story steel moment frame," *Earthq. Eng. Struct. Dyn.*, vol. 40, no. 7, pp. 807–825, Jun. 2011.

[42] D. G. Lignos, T. Hikino, Y. Matsuoka, and M. Nakashima, "Collapse assessment of steel moment frames based on E-Defense full-scale shake table collapse tests," *J. Struct. Eng.*, vol. 139, no. 1, pp. 120–132, 2013.

[43] S. A. Mahin, "Lessons from damage to steel buildings during the Northridge earthquake," *Eng. Struct.*, vol. 20, no. 4–6, pp. 261–270, Apr. 1998.

[44] M. Nakashima, K. Inoue, and M. Tada, "Classification of damage to steel buildings observed in the 1995 Hyogoken-Nanbu earthquake," *Eng. Struct.*, vol. 20, no. 4–6, pp. 271–281, Apr. 1998.

[45] X. Ji, M. Kato, T. Wang, T. Hitaka, and M. Nakashima, "Effect of gravity columns on mitigation of drift concentration for braced frames," *J. Constr. Steel Res.*, vol. 65, no. 12, pp. 2148–2156, Dec. 2009.